Forest Ecology and Management 411 (2018) 35–45

Contents lists available at ScienceDirect

Forest Ecology and Management

journal homepage: www.elsevier.com/locate/foreco

Managing mangrove forests from the sky: Forest inventory using field data and Unmanned Aerial Vehicle (UAV) imagery in the Matang Mangrove Forest Reserve, peninsular Malaysia

Viviana Otero[a,*], Ruben Van De Kerchove[b], Behara Satyanarayana[a,c], Columba Martínez-Espinosa[a], Muhammad Amir Bin Fisol[c], Mohd Rodila Bin Ibrahim[c], Ibrahim Sulong[c], Husain Mohd-Lokman[c], Richard Lucas[d,1], Farid Dahdouh-Guebas[a,e,1]

[a] *Systems Ecology and Resource Management Laboratory, Université Libre de Bruxelles (ULB), Brussels, Belgium*
[b] *Vlaamse Instelling Voor Technologisch Onderzoek (VITO) Research Organisation, Mol, Belgium*
[c] *Mangrove Research Unit, Institute of Oceanography and Environment, Universiti Malaysia Terengganu (UMT), Kuala Terengganu, Malaysia*
[d] *School of Biological, Earth and Environmental Sciences, University of New South Wales (UNSW), Sydney, Australia*
[e] *Laboratory of Plant Biology and Nature Management, Vrije Universiteit Brussel (VUB), Brussels, Belgium*

ARTICLE INFO

Keywords:
UAV
Mangroves
Forest inventory
Structure from Motion
Canopy height model

ABSTRACT

Retrieval of biophysical properties of mangrove vegetation (*e.g.* height and above ground biomass) has typically relied upon traditional forest inventory data collection methods. Recently, the availability of Unmanned Aerial Vehicles (UAV) with different types of sensors and capabilities has proliferated, opening the possibility to expand the methods to retrieve biophysical properties of vegetation. Focusing on the Matang Mangrove Forest Reserve (MMFR) in Perak Province, Malaysia, this study aimed to investigate the use of UAV imagery for retrieving structural information on mangroves. We focused on a structurally complex 90-year-old protective forest zone and a simpler 15-year-old productive forest zone that had been silviculturally managed for charcoal production. The UAV data were acquired in June 2016. In the productive zone, the median tree stand heights retrieved from the UAV and field data were, respectively, 13.7 m and 14 m (no significant difference, p-value = .375). In the protective zone, the median tree stand heights retrieved from the UAV and field data were, respectively, 25.8 and 16.5 m (significant difference, p-value = .0001) taking into account only the upper canopy. The above ground biomass (AGB) in the productive zone was estimated at 217 Mg ha^{-1} using UAV data and 238 Mg ha^{-1} using ground inventory data. In the protective zone, the AGB was estimated at 210 Mg ha^{-1} using UAV data and 143 Mg ha^{-1} using ground inventory data, taking into account only upper canopy trees in both estimations. These observations suggested that UAV data were most useful for retrieving canopy height and biomass from forests that were relatively homogeneous and with a single dominant layer. A set of guidelines for enabling the use of UAV data for local management is presented, including suggestions as to how to use these data in combination with field observations to support management activities. This approach would be applicable in other regions where mangroves occur, particularly as these are environments that are often remote, inaccessible or difficult to work in.

1. Introduction

Forest inventory is a well established approach to support forest monitoring and management (Masek et al., 2015; McRoberts and Tomppo, 2007). However, forest inventory fieldwork is laborious and requires a fine balance between the work objectives and the intrinsic restrictions such as sample size, observation frequency, budget availability and logistical constraints (FAO, 1994; McRoberts and Tomppo, 2007). Recently, there has been an increased usage of remote sensing data involved in the planning, development and implementation of forest inventories as these data can help to overcome some of previously mentioned constraints (FAO, 1994; Masek et al., 2015;

Abbreviations: AGB, above ground biomass; CHM, canopy height model; DSM, digital surface model; MMFR, Matang Mangrove Forest Reserve; RGB, Red Green Blue; SfM, Structure from Motion; UAV, Unmanned Aerial Vehicle

* Corresponding author at: Avenue F.D. Roosevelt 50, CPI 264/1, B-1050 Bruxelles, Belgium.
E-mail address: voterofa@ulb.ac.be (V. Otero).

[1] Authors contributed equally

https://doi.org/10.1016/j.foreco.2017.12.049
Received 20 October 2017; Received in revised form 24 December 2017; Accepted 30 December 2017

McRoberts and Tomppo, 2007).

Mangrove forests are challenging ecosystems in which to perform forest inventory. In addition to the restrictions mentioned above, mangrove forests are typically located in remote and difficult to access areas and surveys are often hindered by tides, mud and dense root networks. Nevertheless, routine monitoring of mangrove forest structure, floristics and biomass is needed for managing resources and ensuring effective conservation and sustainable utilisation. This is particularly important as these forests are one of the most carbon rich in tropical and subtropical regions (Alongi, 2012; Donato et al., 2011; Ha et al., 2017), are an essential component of coastal protection (Dahdouh-Guebas et al., 2005; Othman, 1994; UNEP-WCMC, 2006), maintain biodiversity, are a source of wood, provide livelihood for local populations and procure cultural values (Walters et al., 2008).

Over the past decade, the use of Unmanned Aerial Vehicle (UAV) technology in ecosystem studies has proliferated (Anderson and Gaston, 2013; Pajares, 2015). Common information retrieved from UAV imagery includes plant species, canopy height, stem location, above ground biomass (AGB) and canopy structure (Dandois and Ellis, 2013; Jaskierniak et al., 2016; Messinger et al., 2016; Panagiotidis et al., 2017; Zahawi et al., 2015; Zarco-Tejada et al., 2014; Zhang et al. 2016). UAV technology has the potential to provide a greater amount of spatial information on forest biophysical attributes as it allows more rapid surveys of larger areas compared to more traditional ground-based surveys (Dandois and Ellis, 2013; Messinger et al., 2016; Puliti et al., 2015) and can complement traditional forest inventory techniques (Zahawi et al., 2015; Zhang et al., 2016). Although some studies have used UAVs to study coastal ecosystems (Jaud et al., 2016; Mancini et al., 2013; Wang et al., 2015), the focus on mangrove forests is still limited (Tian et al., 2017).

The research reported here is focused on the Matang Mangrove Forest Reserve (MMFR) in Peninsular Malaysia, which has been managed for more than 100 years, making it the longest managed mangrove reserve in the world (Chong, 2006). The monitoring at MMFR has traditionally been undertaken using ground-based forest inventories (Amir, 2012; Goessens et al., 2014; Gong and Ong, 1995; Putz and Chan, 1986). However, in recent years, different studies have explored the use of remote sensing data (primarily space-borne) and techniques to support the management of the MMFR (Aziz et al., 2015; Hamdan et al., 2013; Hamdan et al., 2014; Ibharim et al., 2015). However, only the studies of Hamdan et al. (2013) and Hamdan et al. (2014) have focused on retrieving biophysical attributes, namely biomass, and none so far have considered forest structure indicators such as tree height. The first objective of this study is to evaluate the use of lightweight UAV technology and Red Green Blue (RGB) images, in combination with ground-based surveys, for retrieving tree height and AGB in the MMFR. A second objective is to develop guidelines for the local management to incorporate the use of UAVs in the routine monitoring of mangroves in the MMFR.

2. Materials and methods

2.1. Study area

The MMFR in Perak State, in peninsular Malaysia, has been managed for pole and charcoal production since 1902 (Chong, 2006). The reserve consists of 40,288 ha of riverine mangrove forest with 27 mangrove species (Fig. 1) (Ariffin and Mustafa, 2013; Chong, 2006). The reserve has a tropical climate and the annual rainfall varies between 2000 and 2800 mm. The monsoons influence the rainfall in the area. Peninsular Malaysia experiences monsoons between November and March (Northeast monsoon) and May and September (Southwest monsoon) (Suhaila and Jemain, 2007). Average air temperature ranges from 22 °C at night to 33 °C during the day (Ariffin and Mustafa, 2013). Tides are semidiurnal and the spring tidal amplitude is 3.3 m (Asthon et al., 1999).

The MMFR is divided in four types of administrative zones: protective (17.4% of the total forest area in the Reserve), productive (74.8%), restrictive productive (6.8%) and unproductive (1%) (Ariffin and Mustafa, 2013). The timber extraction to produce poles and charcoal occurs in the productive and restrictive productive zones. The current silvicultural management consists of a 30 year rotation cycle with two thinnings at 15 and 20 years (Ariffin and Mustafa, 2013). The harvesting is focused on forests dominated primarily by *Rhizophora apiculata* Blume and *R. mucronata* Lamk. Such harvesting results in forest stands that are relatively homogeneous in terms of their species composition, age and biomass. The protective zones are not under the silvicultural management and are areas that support the mangrove forests by providing ecosystem services, including coastal protection, conservation of flora and fauna, and mangrove propagule production. The unproductive zones are lakes and infrastructure, including villages, charcoal kilns and offices (Ariffin and Mustafa, 2013).

2.2. Methods

We followed the workflow outlined in Fig. 2 to evaluate the potential use of UAV to support routine monitoring of the MMFR mangroves. We collected ground and UAV data, processed the data and validated the algorithm for retrieving forest structure characteristics of the mangrove forest.

2.2.1. Data collection

The forest inventory data were collected from two stands in the protective zone and three stands in the productive zone (Fig. 1). The protective zone is not under exploitation and is approximately 90 years old (Goessens et al., 2014; Putz and Chan, 1986). The productive zone is under exploitation and we surveyed 15-year-old forest stands. We chose these two zones because of the differences in forest biophysical characteristics, with one being structurally complex (the protective zone) and the other being more homogeneous (the productive zone). We were not seeking to establish differences in structural measures and AGB between the two stands as a function of forest management, but only to evaluate the performance of the UAV data in two different areas.

Forest inventory data were collected in June, July and December 2016, and April 2017 (Table 1). In each stand, plots were located along a transect perpendicular to the shore running inland from the water margin at 20 m intervals. In each plot, we recorded the species, girth, height and crown diameters for each adult tree (*i.e.* trees with more than 2.5 cm diameter). The species identification of mangroves referenced Tomlinson (1986). Girth was measured using a measuring tape at 130 cm above ground or 30 cm above the highest prop root for *Rhizophora* spp. Height was recorded using a Haga altimeter (error: ± 30 to ± 60 cm per tree). Two crown diameters were measured with a measuring tape, along the north-south and east-west directions. Crown diameters were only recorded in the S1 stands, that is, in the locations where UAV data were also acquired (Table 1). Plot locations were recorded using the Garmin 62stc GPS (± 3.6 m accuracy).

UAV data were acquired using a DJI Phantom 3 Professional quadcopter UAV and the in-built true colour camera in July 2016. Each flight covered an area of at least 1 ha, with both a single parallel and orthogonal flight plan being used (Fig. 3). The flights were planned using Pix4DCapture software and parameterised using a 90% overlap of images to allow subsequent interpolation. Flights were conducted from a boat located approximately 20 m from the forest edge. We included the edge of the water in some of the images even though the water might interfere with the generation of the orthomosaic and derivation of the Digital Surface Model (DSM). Prior to flying, 2.5 m × 2.5 m white tarpaulins were laid out on the ground in three positions inside the area surveyed by the UAV, either within gaps created by lightning strikes or other disturbances. These tarpaulins were used as a zero elevation reference point with which to determine the heights of trees and the

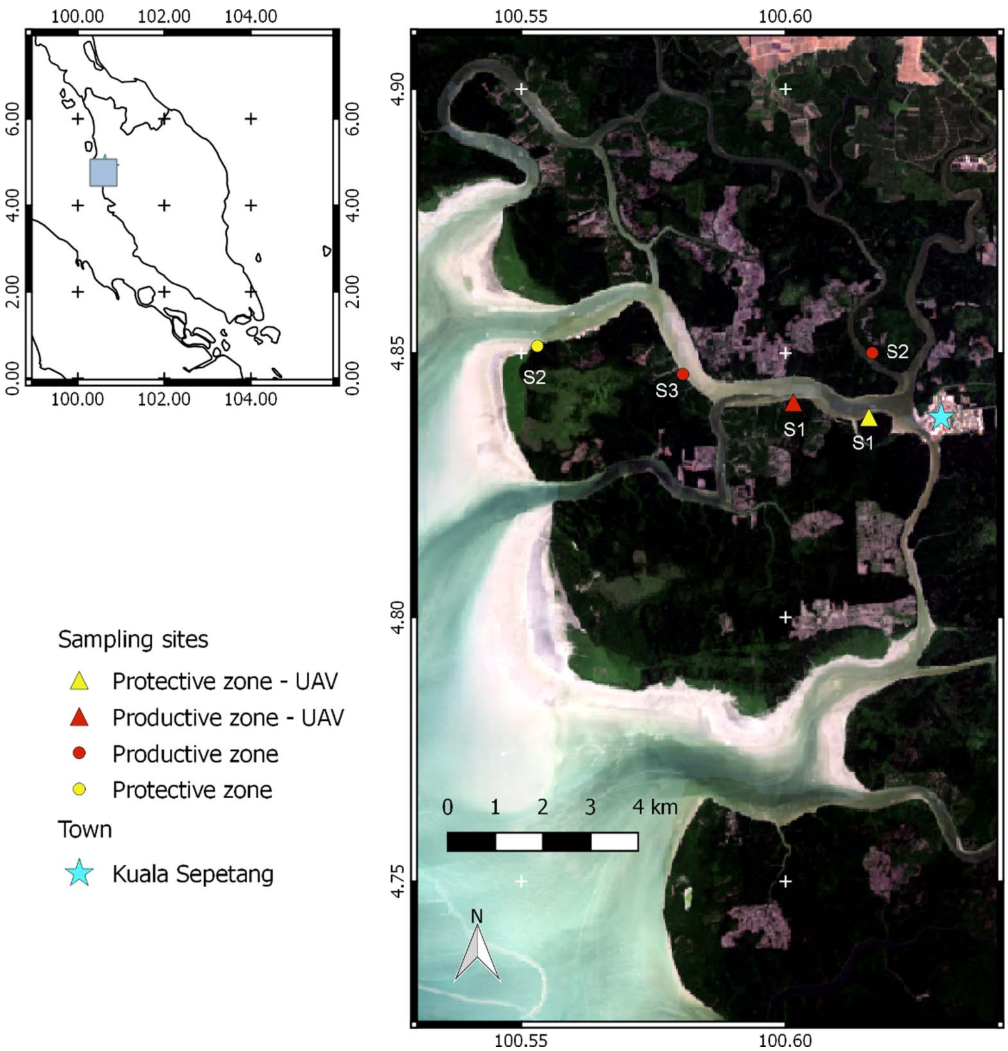

Fig. 1. The MMFR on the west coast of peninsular Malaysia. The present study was conducted in the Kuala Sepetang administrative range. Sampling sites indicated with a triangle correspond to the areas where UAV and inventory data were collected. Sampling sites indicated with a circle correspond to areas where only inventory data were collected. The stand number is indicated as S1, S2 or S3 in each zone. Maps adapted from Weidmann et al. (2010) and Landsat 8 (February 2014) USGS Products.

stand. The flying altitude was on average 109 m.

2.2.2. Data processing

We calculated forest structural descriptors in the productive and protective zones using the inventory data from the S1 stands (Fig. 1). We reported tree density (trees ha^{-1}), basal area ($m^2 ha^{-1}$), AGB (Mg ha^{-1}), diameter and height frequencies, and the relative density (%), relative frequency (%), relative dominance (%) and Importance Value (IV) of each species following standard protocols (Cintron and Novelli, 1984). AGB was estimated at the tree level using the allometric equations provided by Ong et al. (2004) for *R. apiculata* and the common equation for the other mangrove species (Komiyama et al., 2005, 2008), and afterwards scaled up to a unit of Mg ha^{-1} (see Table S1, supplementary information).

We used the Structure from Motion (SfM) technique to create an orthomosaic (3 cm spatial resolution) and a DSM (6 cm spatial resolution) for each stand. The SfM technique creates 3D point clouds based on 2D overlapping photos, using key points in each individual photo to match the same points in another set of photos of the same area (Dittmann et al., 2017; Westoby et al., 2012). Further details on the SfM technique can be found in Westoby et al. (2012) and Dandois and Ellis (2010). We implemented the SfM technique in the Agisoft PhotoScan software and used the UAV GPS data to create the orthomosaics and the DSM as well. Subsequently, Canopy Height Models (CHM) were obtained from the resulting DSM's by subtracting a fixed value, which was determined by visually inspecting the relative height of the tarpaulins and other open areas. The latter approach assumes that little relief is present in the image, which was the case for our study area and also most mangrove areas. This approach also implies that only relative heights are obtained in the CHM, although reference to the tarpaulins at zero elevation provided a more reliable estimation of their actual height.

Tree height was derived from the individual CHMs. The tree height (metres) was determined by applying (i) a Gaussian filter on the CHM and (ii) the tree detection algorithm "FindTreesCHM" available in the package rLiDAR in R (Silva et al., 2015). The "FindTreesCHM" algorithm detects trees by implementing the local maximum function with a fixed window size (Silva et al., 2015). Applying these two procedures required the determination of a window size and a sigma value for the Gaussian filter, and a window size for the tree detection algorithm. Different combinations of these parameters were tested; the sigma value for the Gaussian filter was varied from 0.5 to 18, and the window size for the Gaussian filter and the tree detection algorithm from 5 to 29. To select the best combination of these parameters, we compared the results of the tree detection algorithm with the estimates of tree density based on forest inventory data. We selected two different sets of parameters for each zone. One set corresponded to the total tree density and the second to the trees that were considered to form the upper canopy based on ground inventory data. We selected these trees, as they were the only ones that the UAV would observe, based on tree height and the crown diameters measured in the field. Trees with crowns that were covered by other canopies by at least 50% were excluded. After

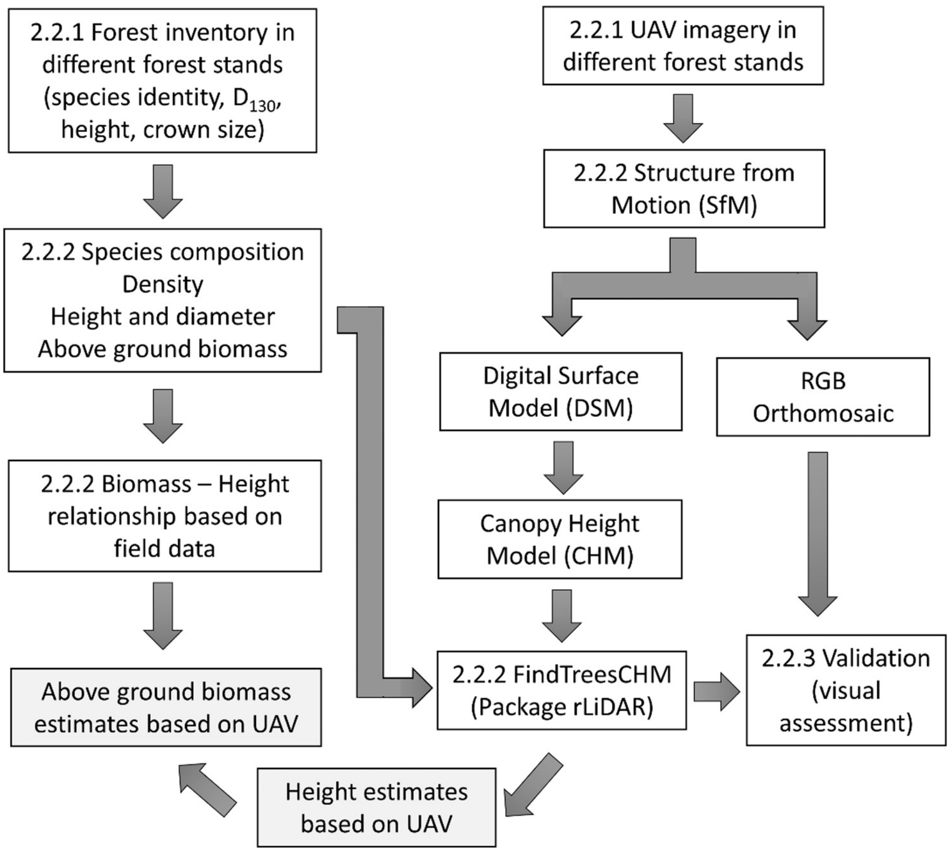

Fig. 2. Workflow to assess the UAV use in MMFR. The left and right sides respectively describe the ground and UAV data collection and processing steps. Numbers refer to the sections in this document.

Table 1
Summary of forest inventory and UAV data collected in the productive and the protective zones in the MMFR. Data collected in the S2 and S3 stands in both zones were used only to calculate the height-biomass relationship (see Section 2.2.2).

Zone	Stand	No. of trees collected	Plot size	Area sampled	UAV imagery available
Productive	S1	35 (in 5 plots)	5 m × 5 m	125 m^2	Yes (1 ha)
	S2	42 (in 3 plots)	10 m × 10 m	300 m^2	No
	S3	108 (in 4 plots)	10 m × 10 m	400 m^2	No
Protective	S1	69 (in 5 plots)	10 m × 10 m	500 m^2	Yes (1 ha)
	S2	52 (in 4 plots)	10 m × 10 m	400 m^2	No
Total	5	306 (in 21 plots)	–	1725 m^2	2 ha

detecting the position of each tree in the CHM using the “FindTreesCHM” algorithm, the height of each tree was retrieved from the CHM.

For the AGB estimation based on the CHM, a quadratic regression was calculated between the height measured in the field and the AGB determined using the allometric equations for each species. We used the data collected in stands S1, S2 and S3 in both productive and protective zones (306 trees). The AGB for each tree detected in the UAV imagery was then estimated using the height retrieved using the CHM. These estimates were then scaled to units of Mg ha^{-1}.

2.2.3. Validation of the tree detection algorithm

We selected the window sizes and the sigma value to apply the “FindTreesCHM” algorithm by comparing the tree counts obtained by the algorithm with the tree density estimations based on forest inventory data. We could not directly compare against the locations of the trees surveyed in the field due to the mismatch in the tree location caused by the combined GPS errors of the UAV and the field GPS. In addition, only the top canopy was observed from the UAV imagery, therefore validation was achieved through visual interpretation of the orthomosaics. The visual interpretation was undertaken by three researchers. Each researcher had to identify single trees in each forest stand from the orthomosaic. In each image, they identified trees within the same plot areas that were sampled during the field campaign. The number of trees identified by each researcher was then compared against the tree count generated by the algorithm. The backgrounds of the three researchers were: (i) an engineer, who was an expert in image processing but with no knowledge of ecology or mangrove forests, (ii) a biologist with advanced knowledge of mangrove forests and with no knowledge of image processing, and (iii) a biologist and expert in mangrove forests with basic knowledge of image processing.

2.2.4. Statistical analyses

Medians of tree height distributions measured in the field and from the UAVs were compared using the Wilcoxon rank test and the normality of each height distribution was tested using a Shapiro-Wilk test. The statistical analyses, the calculation of the quadratic height-biomass relationship and the visual interpretation comparisons were performed in R (R Development Core Team, 2011).

3. Results

3.1. Retrieval of forest structure characteristics using ground inventory data

In total, seven mangrove species were encountered in the productive and the protective zones in sampling zones S1 (Fig. 1). *R. apiculata* and *Bruguiera cylindrica* (L.) Blume were the most abundant in the protective zone, whereas the productive zone was dominated by *R. apiculata* (Table 2).

The protective zone has a larger variation in tree diameter sizes as compared to the productive zone (Fig. 4). Moreover, the productive

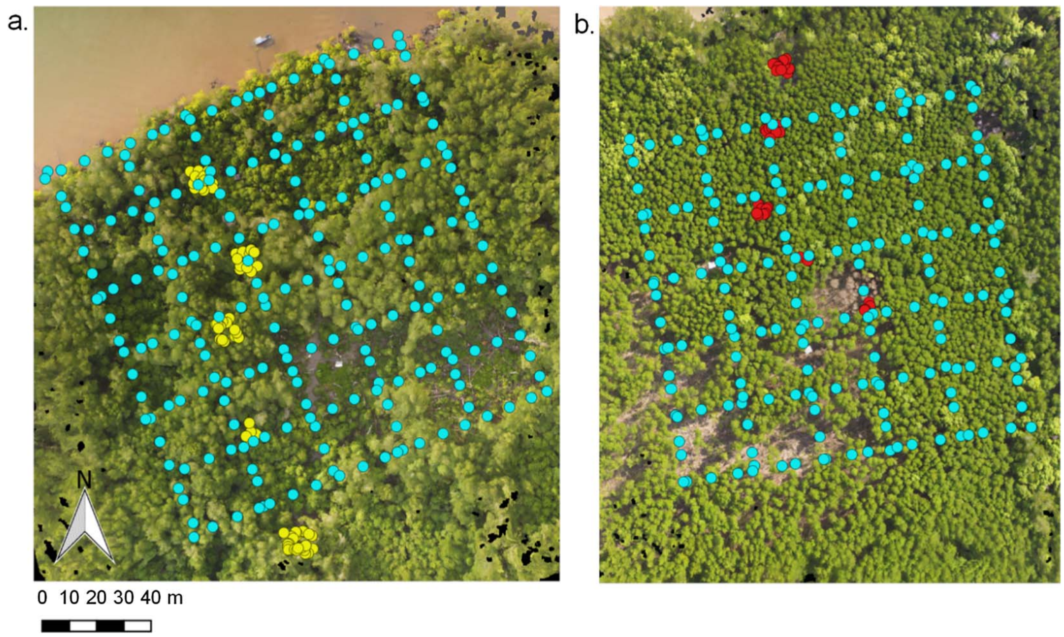

Fig. 3. Diagrammatic representation of the flight plans adopted. The flights over the protective zone S1 (a) and in the productive zone S1 (b) are shown. A picture was taken during the flight in each of the locations indicated in blue. The locations of each tree sampled in the field are shown in yellow (protective zone) and red (productive zone).

zone has a higher density of trees compared to the protective zone (Table 3). Even though the average height in both zones is 14 m, there is more variability of heights in the protective zone. *R. apiculata* was the dominant species in both zones in terms of basal area.

3.2. Orthomosaic images and canopy height Model generation using UAV data

We acquired 191 images in the productive zone and 229 in the protective zone. For each S1 stand, an orthomosaic image, DSM and CHM were generated (Fig. 5). Whereas in the protective zone a more diverse profile of heights was observed, the productive forest was more homogeneous. However, the structural integrity was interrupted by gaps created through lightning strikes.

3.3. Retrieval of forest structure characteristics using UAV data

The parameters to apply the "FindTreesCHM" in the CHM were selected such that the tree density derived from the CHM was as close as possible to the tree density estimated based on the ground inventory data (see Fig. S1 and Table S2 supplementary material). Based on the best set of parameters, the location of each tree was determined in each CHM (Fig. 6). The validation of these results based on visual interpretation are described in the supplementary material (see Table S3 and Fig. S2).

3.3.1. Height estimation using the CHM

When taking into account all the trees measured in the field, the median stand height (25th - 75th percentiles) in the productive zone was 13.7 m (12.6–14.8) and 14 m (11.5–16.5) for UAV and field measurements respectively (Fig. 7a). These two measurements were not significantly different (Wilcoxon rank sum test, p-value = 0.375). When we considered the trees that can only be observed from the top of the canopy, the canopy median heights in the productive zone were 14.2 m (13.1–15) and 15.5 m (13.5–17.5) for UAV and field measurements respectively and were significantly different (Wilcoxon rank sum test, p-value = 0.0066).

In the protective zone, the median stand height estimated based on the UAV data was 25.9 m (15.6–30.3). This value was two times higher than the tree height retrieved from field data when all trees were considered, that is, 12.5 m (8.5–18.5) (Fig. 7b). However, the differences were reduced (by 50%) when taking into account only those trees considered to be part of the upper canopy. The median height retrieved from the UAV data was 25.8 m (14.9–30.5) and 16.5 m (11.2–22.6) from the ground inventory data when only the upper canopy was considered. In this zone, median heights as measured by the UAV were significantly greater than those measured in the field considering all trees (Wilcoxon rank sum test, p-value less than 0.0001) as well as for the trees of the upper canopy (Wilcoxon rank sum test, p-value = 0.0001).

Table 2
Species composition of the protective and productive zones in the S1 forest stands where ground inventory and UAV data were collected. Relative Density (D_{er}), Relative Dominance (D_{or}), Relative frequency (F_r) and Importance Value (IV) are shown.

Species	Productive zone				Protective zone			
	D_{er} (%)	D_{or} (%)	F_r (%)	IV	D_{er} (%)	D_{or} (%)	F_r (%)	IV
Rhizophora apiculata Blume	83	85	63	231	52	78	45	175
R. mucronata Lamk	6	12	13	31	0	0	0	0
Bruguiera parviflora Wight & Arnold ex Griffith	0	0	0	0	41	18	27	86
B. sexangula (Lour.) Poir.	6	2	13	21	0	0	0	0
B. gymnorrhiza (L.) Lamk.	0	0	0	0	1	1	9	11
B. cylindrica (L.) Blume	6	2	13	21	4	2	9	15
Excoecaria agallocha L.	0	0	0	0	1	1	9	11

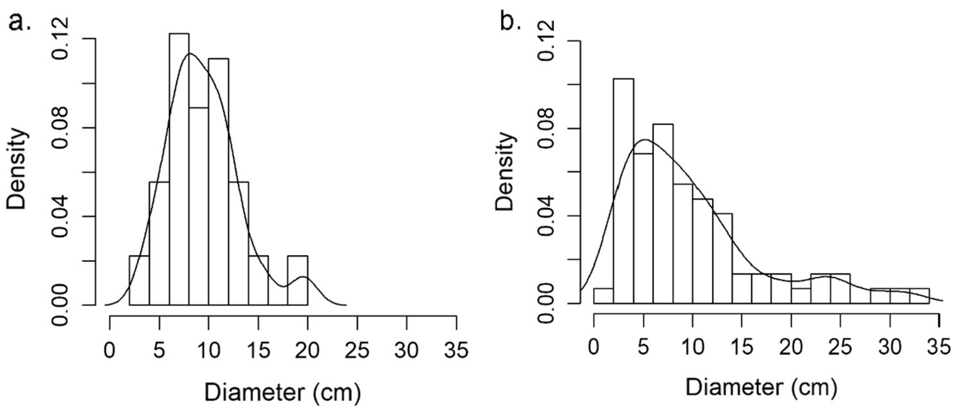

Fig. 4. Diameter frequency histograms. The histograms of the productive (a) and protective (b) zones are shown. Estimated density distributions shown overlaid. All stems of the multi-stemmed trees were considered.

Table 3
Forest structure characteristics in the protective and productive zones in the S1 forest sands where field and UAV data were collected. Average D_{130} and height with their corresponding standard deviation are shown.

Forest structural characteristic	Productive zone	Protective zone
Average D_{130} (cm)	9.5 ± 3.6	9.9 ± 7.2
Average height (m)	14 ± 4	14.1 ± 7.4
Density (trees ha^{-1})	2800	1380
Basal area (m^2 ha^{-1})	*R. apiculata*: 24.5	*R. apiculata*: 13.2
	Other species: 4.4	Other species: 3.8

3.3.2. *Above ground biomass estimation using the CHM*

The quadratic relationship ($R^2 = 0.75$) between AGB and height (H) was determined as (Fig. 8):

$$AGB = 23.5 - 6.5 * H + 0.8 * H^2 \quad (1)$$

In the productive forest, estimated AGB based on the CHM was 217 Mg ha^{-1} which was comparable to that estimated from the ground measurements (238 Mg ha^{-1}) considering all the trees measured in the field (Table 5). In the protective forest, the AGB predicted from the CHM was 442 Mg ha^{-1}, which was 2.6 times more than that generated from the field measurements of all trees (166 Mg ha^{-1}). However, the correspondence in AGB was greater when only those trees forming the upper canopy were observed in both zones (Table 5). In the productive forest, we estimated 143 Mg ha^{-1} compared to the ground estimate of 183 Mg ha^{-1}. In the protective forest, we estimated 210 Mg ha^{-1} using the CHM compared to the ground estimate of 143 Mg ha^{-1}.

4. Discussion

The use of lightweight UAV RGB imagery in combination with the SfM method allowed the generation of orthomosaics and DSM/CHMs for two forest stands in the MMFR. From the CHM, estimates of height and AGB were generated for both forests and there was a close correspondence between CHM derived data and field inventory data for the productive zone (Table 5). Dandois and Ellis (2010), Messinger et al. (2016), Panagiotidis et al. (2017), and Zarco-Tejada et al. (2014) also found that the use of the SfM technique and lightweight UAV can support the retrieval of vegetation structure characteristics. Moreover, the use of the SfM technique to create orthomosaics and CHM is proliferating as UAV use is also increasing and this technique has lower technical requirements as compared to LiDAR (Dandois and Ellis, 2010; Dittmann et al., 2017; Messinger et al., 2016; Panagiotidis et al., 2017; Zahawi et al., 2015).

4.1. *Forest structure characteristics retrieved from the ground forest inventory*

The productive zone is more homogeneous than the protective zone. This is a consequence of the management strategy at MMFR, where stands located in the productive zone are replanted with *R. apiculata* seedlings two years after the clear felling, unless natural regeneration is more than 90% (Ariffin and Mustafa, 2013). Therefore the trees in each stand have similar ages and species composition. The protective zone has not been disturbed for at least 60 years (Putz and Chan, 1986), and accordingly the stand is more heterogeneous in terms of species diversity, tree diameter and tree height.

We found similar tree density and AGB estimates in the productive zone as compared to Goessens et al. (2014) (Table 5). There is an important difference between our estimations and the tree density reported in Gong and Ong (1995). This difference is attributed to two factors. First, the data was collected in a 13-year-old forest stand and second, they collected data in 1980. Although at that time the reserve had the same current management plan, the impact of the previous management strategies on the forest might explain this difference.

In the protective zone, we found different estimations for tree density as compared to Putz and Chan (1986) and Goessens et al. (2014). Putz and Chan (1986) sampled the same area as the present study, but taking into account that 35 years have passed between both sampling campaigns, this difference was expected. Goessens et al. (2014) sampled 21 plots compared to the 5 plots of our study, which can explain the difference in the tree density estimations. This difference in the number of sampling plots is also reflected in the AGB estimates. We found lower AGB estimates compared to Goessens et al. (2014) and Putz and Chan (1986) in the protective zone (Table 5). We sampled 0.05 ha, Goessens et al. (2014) sampled 0.21 ha and Putz and Chan (1986) sampled 0.16 ha.

4.2. *Comparison between forest structure variables retrieved from the ground forest inventory and UAV data*

In the productive zone, the close correspondence between the height and AGB estimates derived from the CHM and the ground inventory data was attributed to the relative homogeneity of the forest (Fig. 4a, Table 5). There was a small (1.3 m) but significant difference between the median height estimates of the UAV and the field inventory data taking into account only the trees from the upper canopy. This difference is attributable in part to the measurement error associated with the Haga Altimeter instrument and to the creation of the CHM using the SfM technique. These results mirror the findings of Panagiotidis et al. (2017), who found a statistically significant difference of 2 m when comparing the height retrieved from a CHM based on the SfM technique and that measured in the field in a temperate forest in the Czech Republic.

In the protective zone, the differences between the height estimates based on UAV and based on ground inventory, are a result of the heterogeneity of the forest (Fig. 4b). There is more variation in the species composition, as well as in the diameter and height classes in this zone.

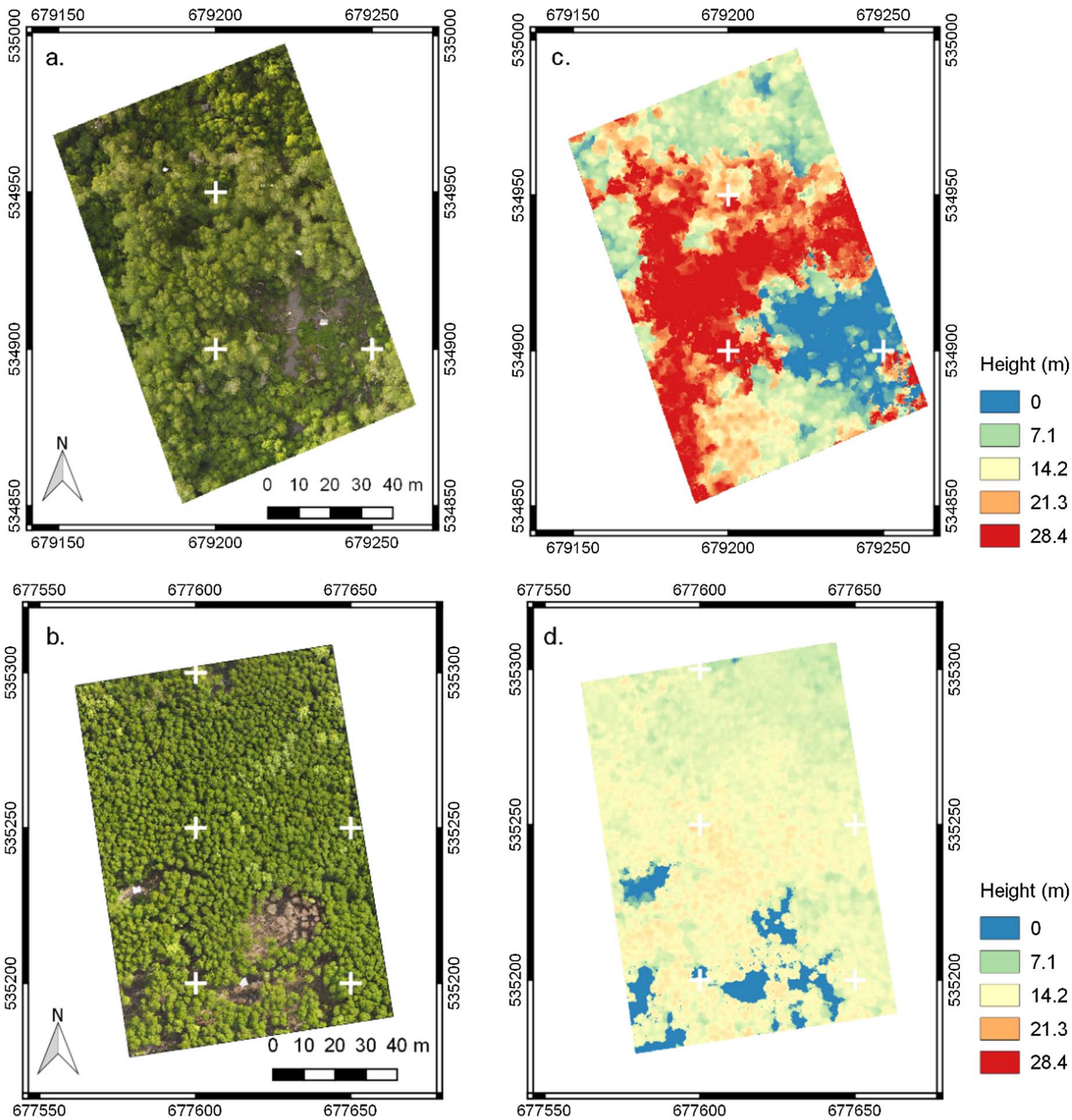

Fig. 5. UAV data derived products. Orthomosaic images of the protective zone (a) and the productive zone (b). CHM generated for the protective zone (c), and the productive zone (d).

Although there was a significant difference in the height estimations in this zone, the tree height estimates based on the CHM and measured in the field were comparable only when considering larger trees. Concerning the AGB estimates, better results were obtained when retaining only the trees observed from the top of the canopy (Table 5). When all trees were considered, the AGB was overestimated as the height estimates for the protective zone were larger than the heights measured in the field. Therefore, when using the quadratic relationship between height and AGB, larger AGB estimates resulted as only the tallest trees of the zone were used for scaling.

The ability to link forest structure variables retrieved from UAV data to field measurements opens the possibility to further explore other forest age stands that are under management and therefore are of similar species composition and height homogeneity. If it is possible to obtain a useful height estimation in the exploitable areas of the reserve, local managers may then have a better estimate of height distributions and the AGB of the stands, offering valuable information that can support better timber extraction practices. Bendig et al. (2014), Messinger et al. (2016) and Zahawi et al. (2015) also found that the use of lightweight UAV and the SfM technique can be used as a tool to estimate AGB and therefore support local management and monitoring of crops and tropical forests.

4.3. Strengths and limitations of the present study

This study has three major strengths. (i) To the best of our knowledge, this is the first study where lightweight UAVs have been used to retrieve information on the tree height and AGB of mangrove forests. (ii) The ground forest inventory and UAV data were collected at the same time and in the same location. (iii) The methods and results of this study are accessible and available to support the local management of the MMFR.

This study has three major limitations. (i) The methods used are suitable for monitoring the productive zones of the reserve but there are shortcomings for the protective zones. The protective zones are more heterogeneous and the sub-canopy is generally not observed within optical data, which limits the retrieval of forest structure characteristics in these areas. (ii) The UAV data were collected on only one occasion in

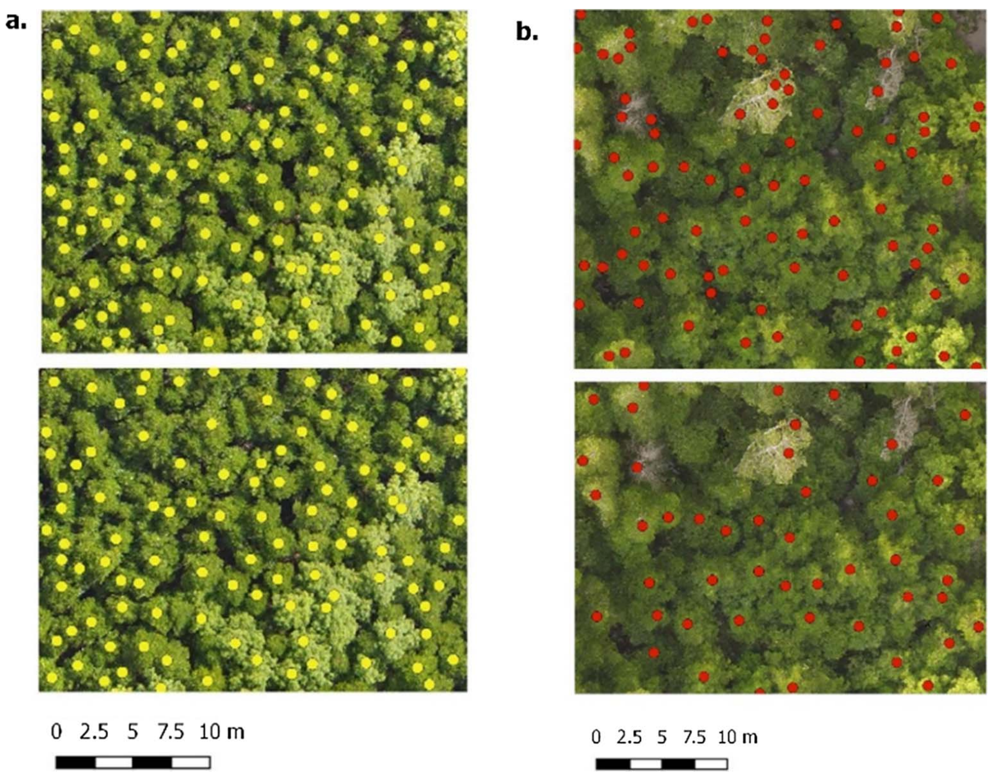

Fig. 6. Trees detected in the CHM. Example of the location of the trees detected by the algorithm in the productive zone (a) and in the protective zone (b). The upper image correspond to the set of parameters using all the trees measured in the field, and the bottom image correspond to the parameters using only the trees that form the upper canopy (see Table S2, supplementary material).

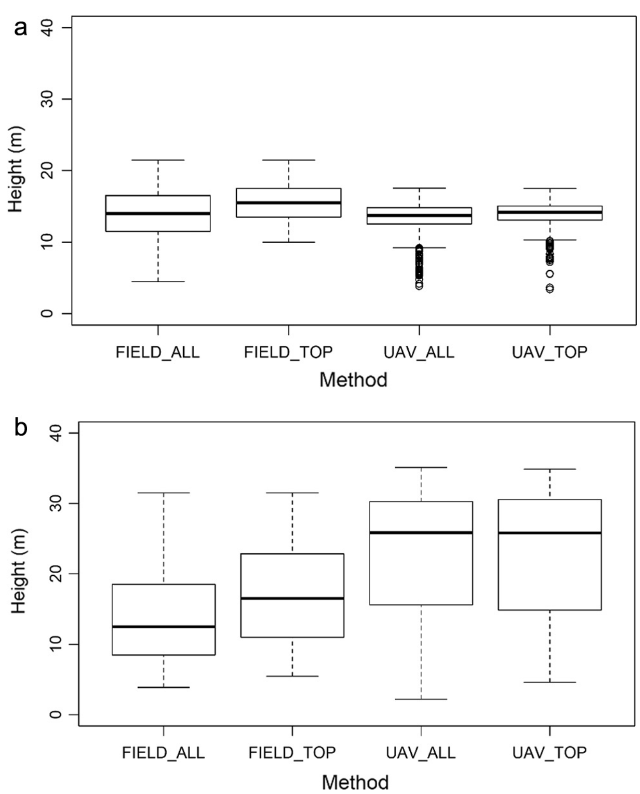

Fig. 7. Comparisons between the height retrieved from the field inventory and the CHM. The correspondence between canopy height measured in the productive (a) and in the protective zone (b) is shown. The heights measured in the field including all the trees are indicated with “FIELD_ALL”, the heights including only the trees observed from the top of the canopy are indicated with “FIELD_TOP”. The heights retrieved from the CHM using the parameters based on all the trees from the field inventory are indicated as “UAV_ALL” and the heights retrieved using the parameters based on only the upper canopy trees are indicated by “UAV_TOP”.

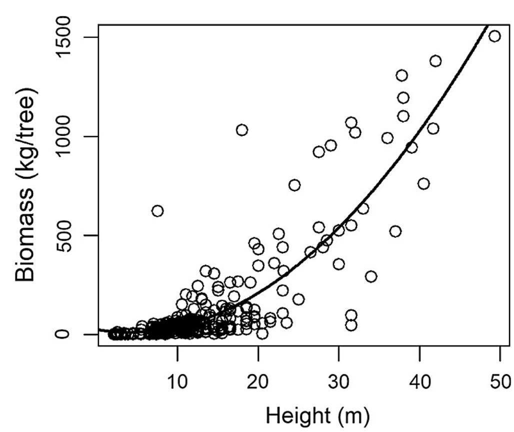

Fig. 8. Quadratic relationship between AGB and height. Relationship is based on ground inventory data collected in the stands S1, S2 and S3 located in productive and protective zones (see locations in Fig. 1).

each stand because of logistical constraints. Repeated measurements were not considered necessary because the mangrove forests are evergreen and hence do not experience a large amount of seasonal variation in leaf and canopy cover. However, repeated measurements over time and on an annual basis would be useful to track changes in the structure, floristic composition and AGB of mangrove forests that are both protected or managed for commercial purposes. This was however beyond the scope of the present study. (iii) The tree detection algorithm provides a reasonable approximation of tree density, but is of limited use for location of some single trees in both zones. A tree crown might have several high points and not necessarily a round shape. Even by visual inspection, tree identification in the orthomosaics proved challenging (see supplementary material Fig. S2, Table S3); although tree counts made by visual inspection corresponded to those by the tree detection algorithm when only the upper canopy was considered (R^2 = 0.6, p-value = 0.0088). Nevertheless, improvements in current tree detection algorithms are needed, specially to increase their

Table 5
Summary forest structure characteristics estimated in this study using the field inventory data and the CHM based on the UAV data. Results from other studies based on forest inventory data in the same reserve are also shown: (i) Goessens et al. (2014), (ii) Gong and Ong (1995) - comparison with a 13-year-old forest stand -, and (iii) Putz and Chan (1986). AGB estimations in this study included all species whilst other studies only considered *R. apiculata*.

Parameter	Zone	Field inventory data	CHM (all trees)	CHM (top trees)	Other studies
Tree density (tree ha^{-1})	Productive	2800 (all trees) 1600 (top trees)	2562	1578	2236 (i) 9250 (ii)
	Protective	1380 (all trees) 660 (top trees)	1243	596	2283 (i) 681 (iii)
Median height (m)	Productive	14 (all) 15.5 (top)	13.7	14.2	12.6 (i)
	Protective	12.5 (all) 16.5 (top)	25.9	25.8	9.7 (i)
AGB (Mg ha^{-1})	Productive	238 (all) 183 (top)	217	143	216 (i) 131 (ii)
	Protective	166 (all) 143 (top)	442	210	415 (i) 270–460 (iii)

usability by non-experts of remotely sensed imagery processing.

4.4. Benefits and limitations of using UAV data for inventory of mangrove forests

The brief time required to sample one hectare of forest is one of the main advantages of the use of UAVs for vegetation monitoring. The UAV data acquisitions, including flight planning and set up, took no more than 1 h in one sampling site. The flight typically took less than 12 min and covered an area of approximately one hectare of forest. Three people were involved in the execution of the flights. In contrast, for the ground forest inventory, three people with experience in field sampling worked two complete days (approximately 7 h day^{-1}) to sample 5 percent of a hectare of mangrove forest.

The UAV facilitates access to areas that are difficult to reach by foot. The UAV was launched from both land and from a boat, which allowed flights to be conducted in areas that were difficult to enter, particularly at very high or low tides. Moreover, the frequency of forest monitoring can be increased with a combination of ground and UAV inventory. Traditional inventory is still required in spite of the availability of new technologies as UAV. Nevertheless, due to the poor accessibility and the effort required to perform a traditional ground forest inventory, sampling is not frequently executed in the reserve. With a combination of both approaches, the MMFR forest could be monitored more frequently. Furthermore, the use of UAV to monitor forests does not disturbs the fauna and flora of the sampled area as much as traditional inventory surveys. UAV observations also provided a unique insight and a historical record with capacity for near real time reporting and validation of change events and processes in the forest.

We suggest technology and image processing methods that are accessible for the local Forestry Department, who manages the MMFR. We used a lightweight UAV with an RGB camera (around € 1200) that is easy to operate after a short training. Although we used AgiSoft Photoscan to generate the DSM and CHM, there are open source alternatives available such as Ecosynth (Dandois and Ellis, 2010). Additionally, the workflow and guidelines presented in this study can be used by the local Forestry Department as a protocol for the use of these technologies to monitor, manage and report on the condition of the MMFR. Whilst the application of the protocol requires technical training, it will also empower the local managers and support a better management of the forest (Paneque-Galvez et al., 2014).

A limitation of this approach is that only the upper canopy is observed. However this limitation mostly affected information extraction from the protective forest. Conversely, in the productive forest, height and AGB can be estimated well and it is therefore feasible to provide important information on the areas where timber extraction occurs.

Other limitations are associated with increasing concerns of security and ethical implications in the use of UAV for conservation purposes (Paneque-Galvez et al., 2014; Sandbrook, 2015). These concerns are reflected in the increasing legislation regulating UAV use in different countries (Nex and Remondino, 2014; Sandbrook, 2015). Though the benefits of using UAV for monitoring are clear, an appropriate introduction to the community and the compliance of local legislation are basic for proper UAV use in conservation or monitoring purposes. In Malaysia, the regulation for UAV of less than 20 kg establishes that a flight certification is not necessary. Nevertheless, there are restricted flying areas, the maximum flight altitude is 122 m (400 feet) and the aircraft operator must have an insurance in case of an accident (Aeronautical Information Services, 2008). At all times, consideration needs to be given to regulations and to the aircraft.

4.5. Guidelines for UAV flights and image processing for the local management

Based on the experience at the MMFR, the following recommendations are given for UAV data acquisitions in mangrove areas:

i. Flights should be at an altitude of approximately 40 m above the estimated maximum height of the canopy (Dandois and Ellis, 2013).
ii. To cover an area of 1 ha (*e.g.* 100 m × 100 m), flights need to be planned such that they cover an area that is at least 20% greater (*e.g.* 120 m × 120 m) to be able to remove the distortion at the borders (Dandois and Ellis, 2013).
iii. Areas of water should be excluded as this leads to errors in the detection of the same features in stereo pairs and in the interpolation (Westoby et al., 2012). However, care needs to be taken if the mangrove margin needs to be captured.
iv. Acquisitions should ideally be at low (and preferably on the incoming) tide as water may compromise the generation of the orthomosaic and the CHMs.
v. Tarpaulins should ideally be placed in open areas and in three locations positioned as a triangle, as this allows more reliable estimation of tree and stand heights.
vi. The flight should be planned such that it follows an orthogonal pattern of flying and a 90% overlap of the images, which facilitates better matching of the component images. Forward overlaps exceeding 90% have also been used by Dandois and Ellis (2013) and Zahawi et al. (2015).
vii. For the retrieval of biophysical properties of mangroves, we recommend the workflow shown in Fig. 2. The selection of the parameters required to implement "FindTreesCHM" can be undertaken through reference to ground inventory data, which can be acquired alongside UAV data collections and at lower frequencies. Additionally, it is necessary to define a different set of parameters for the tree detection algorithm for each sampling area as the species composition and homogeneity of the forest in each area may vary.

5. Conclusions

In this study we demonstrated that lightweight UAVs can be used to support the monitoring of the mangrove forest in the MMFR. We were able to estimate tree height and AGB in the productive zone using UAV data that had a close correspondence to the estimates based on ground forest inventory. Therefore, valuable information can be generated for the local management, especially in areas where timber extraction occurs.

The use of UAV data in mangroves studies can lead to significant advances in quantifying forest growth stages and changes over time. It can also increase the frequency of monitoring and complement traditional forest inventory. Therefore, this study recommends elements of UAV planning and acquisition in the development of protocols for mangrove surveys. We also present guidelines for the local management to incorporate this technology in the regular monitoring of the MMFR.

Acknowledgements

We would like to thank the Perak State Forestry Department and the local rangers of the MMFR for their support during the fieldwork, in particular, to ranger Pak Abu. We would also like to thank Emilia Ashari, for her collaboration during the fieldwork, and Dries Raymaekers, for the UAV training sessions and expertise to plan the UAV flights. Furthermore, Fabian Güiza and Fleur Van Nedervelde contributed with the visual interpretation of the orthomosaic images. This study was carried with the approval of the Perak State Forestry Department, Ipoh, Malaysia.

Funding acknowledgements

The research presented in this paper is funded by BELSPO (Belgian Science Policy Office) in the frame of the STEREO III Programme – Project Managing Mangrove Forests with Optical and Radar Environmental Satellites (MAMAFOREST) (SR/00/323).

Conflicts of interest

None.

Appendix A. Supplementary material

Supplementary data associated with this article can be found, in the online version, at http://dx.doi.org/10.1016/j.foreco.2017.12.049.

References

Aeronautical Information Services (AIC) (2008). Unmanned Aerial Vehicle (UAV) operations in malaysian airspace. Retrieved from http://aip.dca.gov.my/aip%20pdf%20new/AIC/AIC%20200804.pdf [retrieved on June 2017].

Alongi, D.M., 2012. Carbon sequestration in mangrove forests. Carbon Manage. 3 (3), 313–322. http://dx.doi.org/10.4155/cmt.12.20.

Amir, A.A., 2012. Canopy gaps and the natural regeneration of Matang mangroves. Forest Ecol. Manage. 269, 60–67. http://dx.doi.org/10.1016/j.foreco.2011.12.040.

Anderson, K., Gaston, K.J., 2013. Lightweight unmanned aerial vehicles will revolutionize spatial ecology. Front. Ecol. Environ. 11 (3), 138. http://dx.doi.org/10.1890/120150.

Ariffin, R., Mustafa, N.M.S.N., 2013. A Working Plan for the Matang Mangrove Forest Reserve, Perak (6th revision). State Forestry Department, Malaysia.

Asthon, E.C., Hogart, P.J., Ormond, R., 1999. Breakdown of mangrove leaf litter in a managed mangrove forest in Peninsular Malaysia. Hydrobiologia 413, 77–88. http://dx.doi.org/10.1023/A:1003842910811.

Aziz, A.A., Pinn, S., Dargusch, P., 2015. Investigating the decline of ecosystem services in a production mangrove forest using Landsat and object-based image analysis. Estuar. Coast. Shelf Sci. 164, 353–366. http://dx.doi.org/10.1016/j.ecss.2015.07.047.

Bendig, J., Bolten, A., Bennertz, S., Broscheit, J., Eichfuss, S., Bareth, G., 2014. Estimating Biomass of Barley Using Crop Surface Models (CSMs) Derived from UAV-Based RGB Imaging. Remote Sensing 6, 10395–10412. http://dx.doi.org/10.3390/rs61110395.

Chong, V.C., 2006. Sustainable utilization and management of mangrove ecosystems of Malaysia. Aquatic Ecosyst. Health Manage. 9 (2), 249–260.

Cintron, G., Novelli, Y.S., 1984. Methods for studying mangrove structure. In: Snedaker, S.C., Snedaker, J.G. (Eds.), The Mangrove Ecosystem: Research Methods. UNESCO, Paris, pp. 91–113.

Dahdouh-Guebas, F., Jayatissa, L.P., Di Nitto, D., Bosire, J.O., Seen, D.L., Koedam, N., 2005. How effective were mangroves as a defence against the recent tsunami? Current Biol. 15 (12), R443–R447. http://dx.doi.org/10.1016/j.cub.2005.06.008.

Dandois, J., Ellis, E.C., 2010. Remote sensing of vegetation structure using computer vision. Rem. Sens. 2, 1157–1176. http://dx.doi.org/10.3390/rs2041157.

Dandois, J., Ellis, E.C., 2013. High spatial resolution three-dimensional mapping of vegetation spectral dynamics using computer vision. Remote Sens. Environ. 136, 259. http://dx.doi.org/10.1016/j.rse.2013.04.005.

Dittmann, S., Thiessen, E., Hartung, E., 2017. Applicability of different non-invasive methods for tree mass estimation:a review. For. Ecol. Manage. 398, 208–215. http://dx.doi.org/10.1016/j.foreco.2017.05.013.

Donato, D.C., Kauffman, J.B., Murdiyarso, D., Kurnianto, S., Stidham, M., Kanninen, M., 2011. Mangroves among the most carbon-rich forest in the tropics. Nat. Geosci. 4, 293–297. http://dx.doi.org/10.1038/ngeo1123.

FAO, 1994. Mangrove forest management guidelines. FAO Forestry Paper 117, 110.

Goessens, A., Satyanarayana, B., Van der Stocken, T., Quispe Zuniga, M., Moh-Lokman, H., Sulong, I., Dahdouh-Guebas, F., 2014. Is Matang Mangrove Forest in Malaysia sustainably rejuvenating after more than a century of conservation and harvesting management? PLoS One 9 (8). http://dx.doi.org/10.1371/journal.pone.0105069.

Gong, W.K., Ong, J.E., 1995. The use of demographic studies in mangrove silviculture. Hydrobiologia 195, 255–261. http://dx.doi.org/10.1007/978-94-011-0289-6_29.

Ha, T.H., Marchand, C., Aime, J., Nhon, Dang Hoai, Hong, Phan Nguyen, Tung, Nguyen Xuan, Cuc, Nguyen Thi Kim, 2017. Belowground carbon sequestration in a mature planted mangroves (Northern Viet Nam). For. Ecol. Manage. http://dx.doi.org/10.1016/j.foreco.2017.06.057.

Hamdan, O., Khairunnisa, M., Ammar, A., Hasmadi, I., Aziz, H., 2013. Mangrove carbon stock assessment by optical satellite imagery. J. Trop. For. Sci. 25 (4), 554–565.

Hamdan, O., Kahali Aziz, H., Mohd Hasmadi, I., 2014. L-band ALOS PALSAR for biomass estimation of Matang Mangroves, Malaysia. Remote Sens. Environ. 155, 69–78.

Ibharim, N.A., Mustapha, M.A., Lihan, T., Mazlan, A.G., 2015. Mapping mangrove changes in the Matang Mangrove Forest using multi temporal satellite imageries. Ocean Coast. Manage. 114, 64–76.

Jaskierniak, D., Kuczera, G., Benyon, R.G., Lucieer, A., 2016. Estimating tree and stand sapwood area in spatially heterogeneous southeastern Australian forests. J. Plant Ecol. 9 (3), 272.

Jaud, M., Grasso, F., Le Dantec, N., Verney, R., Delacourt, C., Ammann, J., Deloffre, J., Grandjean, P., 2016. Potential of UAVs for Monitoring mudflat morphodynamics (applications to the Seine Estuary, France). Int. J. Geo-Inform. 5 (50). http://dx.doi.org/10.3390/ijgi5040050.

Komiyama, A., Poungparn, S., Kato, S., 2005. Common allometric equations for estimating the tree weight of mangroves. J. Trop. Ecol. 21, 471–477.

Komiyama, A., Ong, J.E., Poungparn, S., 2008. Allometry, biomass and productivity of mangrove forest: a review. Aquat. Bot. 89, 128–137.

Mancini, F., Dubbini, M., Gattelli, M., Stecchi, F., Fabbri, S., Gabbianelli, G., 2013. Using Unmanned Aerial Vehicles (UAV) for high-resolution reconstruction of topography: the structure from motion approach on Coastal Environments. Remote Sens. 5, 6880.

Masek, J.G., Hayes, D.J., Hughes, M.J., Healey, S.P., Turner, D.P., 2015. The role of remote sensing in process-scaling studies of managed forest ecosystems. For. Ecol. Manage. 355, 109–123.

Messinger, M., Gregory, P., Asner, G.P., Silman, M., 2016. Rapid assessment of Amazon forest structure and biomass using small unmanned aerial systems. Remote Sens. 8, 615. http://dx.doi.org/10.3390/rs8080615.

McRoberts, R.E., Tomppo, E.O., 2007. Remote sensing support for national forest inventories. Remote Sens. Environ. 110 (4), 412–419. http://dx.doi.org/10.1016/j.rse.2006.09.034.

Nex, F., Remondino, F., 2014. UAV for 3D mapping applications: a review. Appl Geomat 6, 1–15. http://dx.doi.org/10.1007/s12518-013-0120-x.

Ong, J.E., Gong, W.K., Wong, C.H., 2004. Allometry and partitioning of the mangrove Rhizophora apiculata. For. Ecol. Manage. 395–408.

Othman, M.A., 1994. Value of mangroves in coastal protection. Hydrobiologia 285, 277–282. http://dx.doi.org/10.1007/BF00005674.

Pajares, G., 2015. Overview and current status of remote sensing applications based on unmanned aerial vehicles (UAV). Photogramm. Eng. Remote Sens. 81 (4), 281–329.

Panagiotidis, D., Abdollahnejad, A., Surovy, P., Chiteculo, V., 2017. Determining tree height and crown diameter from high-resolution UAV imagery. Int. J. Remote Sens. 38 (8–10), 2392–2410. http://dx.doi.org/10.1080/01431161.2016.1264028.

Paneque-Gálvez, J., McCall, M.K., Napoletano, B.M., Wich, S.A., Koh, L.P., 2014. Small drones for community-based forest monitoring: an assessment of their feasibility and potential in tropical areas. Forests 5, 1481.

Puliti, S., Ole Orka, H., Gobakken, T., Naesset, E., 2015. Inventory of small forest areas using an unmanned aerial system. Rem. Sens. 7, 9632.

Putz, F.E., Chan, H.T., 1986. Tree growth, dynamics, and productivity in a mature mangrove forest in Malaysia. For. Ecol. Manage. 17, 211–230.

R Development Core Team. R: A language and environment for statistical computing. Austria: R Foundation for Statistical Computing Vienna, 2011.

Sandbrook, C., 2015. The social implications of using drones for biodiversity conservation. Ambio 44, S636–S647.

Silva. C.A., Crookston, N.L., Hudak, A.T. and Vierling, L.A., 2015. Package 'rLiDAR': LiDAR Data Processing and Visualization. Available in CRAN repository. Retrieved from https://cran.r-project.org/web/packages/rLiDAR/rLiDAR.pdf (May 2017).

Suhaila, J., Jemain, A.A., 2007. Fitting daily rainfall amount in Malaysia using the normal transform distribution. J. Appl. Sci. 7 (14), 1880–1886.

Tian, J., Wang, L., Li, X., Gong, H., Shi, C., Zhong, R., Liu, X., 2017. Comparison of UAV and WorldView-2 imagery for mapping leaf area index of mangrove forest. Int. J. Appl. Earth Observ. Geoinform. 61, 22–31.

Tomlinson, P.B., 1986. The Botany of Mangroves. Cambridge University Press, Cambridge, pp. 419.

UNEP-WCMC, 2006. In the Front Line: Shoreline Protection and other Ecosystem Services from Mangroves and Coral Reefs, 33. UNEP-WCMC, Cambridge.

Walters, B.B., Rönnbäck, P., Kovacs, J.M., Crona, B., Hussain, S.A., Badola, R., Primavera, J.H., Barbier, E., Dahdouh-Guebas, F., 2008. Ethnobiology, socio-economics and management of mangrove forest: a review. Aquat. Bot. 89, 220–236.

Wang, A., Chen, J., Jing, C., Ye, G., Wu, J., Huang, Z., Zhou, C., 2015. Monitoring the Invasion of Spartina alterniflora from 1993 to 2014 with Landsat TM and SPOT 6 Satellite Data in Yueqing Bay, China. PLoS One 10 (8), e0135538. http://dx.doi.org/

10.1371/journal.pone.0135538.
Weidmann, Nils B., Kuse, Doreen, Gleditsch, Kristian Skrede, 2010. The geography of the international system: the CShapes dataset. Int. Interact. 36 (1).
Westoby, M.J., Brasington, J., Glasser, N.F., Hambrey, N.J., Reynolds, J.M., 2012. 'Structure-from-Motion' photogrammetry: a low-cost, effective tool for geoscience applications. Geomorphology 179, 300–314.
Zahawi, R.A., Dandois, J.P., Holl, K.D., Nadwodny, D., Reid, J.L., Ellis, E.C., 2015. Using lightweight unmanned aerial vehicles to monitor tropical forest recovery. Biol. Conserv. 186, 287.
Zarco-Tejada, P.J., Diaz-Varela, R., Angileri, V., Loudjani, P., 2014. Tree height quantification using very high resolution imagery acquired from an unmanned aerial vehicle (UAV) and automatic 3D photo-reconstruction methods. Eur. J. Agron. 55, 89–99. http://dx.doi.org/10.1016/j.eja.2014.01.004.
Zhang, J., Hud, J., Liane, J., Fan, Z., Ouyang, X., Ye, W., 2016. Seeing the forest from drones: Testing the potential of lightweight drones as a tool for long-term forest monitoring. Biol. Conserv. 198, 60.